Minimum mass laminate design for uncertain in-plane loading

Mark W. D. Nielsen[1], Richard Butler[1], and Andrew T. Rhead[1,2]

[1]*Materials and Structures Research Centre, Department of Mechanical Engineering, University of Bath, Claverton Down Road, Bath, Somerset, BA2 7AY, United Kingdom*

[2]*Corresponding Author: Email: A.T.Rhead@bath.ac.uk*

Abstract (100-150 words)

Requirements for lower emissions and operating costs make mass reduction of composite structures a significant issue for future aircraft. Here, minimisation of normalised elastic energy under an uncertain, general in-plane loading is used to indicate laminate efficiency and by equivalence minimum mass. Results are the first to investigate the comparative robustness of standard and non-standard angles to uncertain loading. They indicate that weight reductions of up to 8% can be achieved if optimum design, using standard angle (θ = 0°, ±45° or 90°) and industrial design rules, is replaced by optimising non-standard angles ($0° \leq \theta \leq 180°$) directly for uncertain loading. However, greater reductions of up to 20% are possible through alignment of laminate balancing axes with principal loading axes. As such, a non-standard angle design strategy is only shown to be warranted if the demonstrated non-uniqueness of optimum designs can be exploited to improve other performance drivers.

Keywords: A: *Laminates; B: Strength; C: Laminate mechanics; Robust design*

1. Introduction

Minimum mass aerospace laminate design is a multi-constraint problem. All relevant failure modes such as buckling, damage tolerance, bolt bearing and notched strength should be considered in order to produce a minimum mass design that delivers the required performance. However, such a complex approach is not justified in the initial design stage. Netting analysis, which ignores the support of the resin matrix and aligns fibres in principal directions to carry principal stresses, leads to laminate designs in which the stresses in fibres are limited to some value associated with failure i.e. fully-stressed fibre design. Verchery [1] has shown that Netting analysis, can be treated as a limiting case of Classical Laminate Theory. His approach indicates that designs with fewer than three fibre directions produce mechanisms when subject to small disturbances in loading. This reveals the reasoning behind established aerospace laminate design practice of using four standard angles (SAs) (0°, +45°, -45° and 90°) and a

design rule of a 10% minimum ply percentage to provide a level of redundancy against loading uncertainty [2]. In contrast, non-standard angle (NSA) designs permit the use of all possible fibre angles ($0° \leq \theta \leq 180°$) providing greater scope for stiffness tailoring. The advantages of tailoring have been demonstrated through use of lamination parameters and NSA layups over quasi-isotropic layups in optimisation procedures of wing structure solutions for aero-elastic tailoring purposes [3,4], for increased panel buckling performance [5,6], as well as enabling certain types of stiffness couplings [7]. NSAs have also been extensively studied for their use in winding angles for optimising pressure vessel strength [8,9]. However, a lack of specific design rules for NSA laminates can lead to optimum aerostructure designs for specific loadings that, in the extreme Netting analysis regime context, form mechanisms with any perturbation in load. Such laminates rely on the weak resin matrix to prevent collapse under a varying load state. In this paper, to avoid problems of robustness, both NSA and SA laminates are designed considering an uncertain in-plane loading with the use of anti-optimisation, allowing design all loading scenarios that could be applied. This ensures the structure is designed for the worst case loading i.e. the critical condition limiting the mass of the structure under consideration. Anti-optimisation describes the min-max or max-min optimisation technique whereby a design is optimised to have the best possible worst case performance for the range of uncertainties considered [10] e.g. maximising the minimum buckling load from the range of loads that could be applied from a defined uncertainty in loading, as is the case in Adali et al. [11]. The authors found that, a deterministic design is seen to underperform in buckling performance compared to a robust design when uncertain loads are applied. Anti-optimisation is usually a two-step optimisation process with one optimisation nested within the other [10]. However, here the worst case performance for a range of loadings is found analytically, similar work is also shown by Adali for buckling design under uncertain in-plane loads [12]. Composite laminate uncertainties are also associated with the material and the manufacturing process [12,13] but this not considered in this paper. Optimising for a loading uncertainty has the potential to replace the requirement for a 10% minimum ply percentage rule in SA designs and allows the use of NSAs without an equivalent constraint. An equivalent NSA 10% rule has been applied by Abdalla et al. [14] using the in-plane lamination parameter space to allow a selection of designs which have a base stiffness in all directions. Similarly a technique ensuring a minimum degree of isotropy in NSA laminate optimisations is shown by Peeters and Abdalla [15] ensuring robust laminates. However, instead of an identical robustness in all directions, the robustness of a design may be better tailored if the range of loads that could be applied are known.

In order to compare design approaches that use SAs and NSAs, laminate in-plane elastic energy under combined bi-axial and shear loading is used to assess laminate efficiency in this paper. Elastic energy minimisation or compliance energy minimisation is a computationally efficient technique that uses either topology or orientation of materials with directional properties, to produce the structures with maximum efficiency. Structures with optimum efficiency take advantage of directional material stiffness properties to produce a minimum global strain state. This requires the structure to have the greatest global stiffness for a given volume of material. Prager and Taylor [16] first outlined optimality criteria justifying the technique of minimisation of elastic energy (subject to given loads) to produce a structure with optimal efficiency. Pedersen [17] subsequently applied this technique to composite materials to find analytical solutions for orientation of a single ply angle subject to in-plane loading. Solutions for multi-layered anisotropic laminates are provided for tri-axial design loadings. Minimisation of in-plane elastic energy in laminate design does not directly imply maximisation of in-plane strength of a composite material. Nevertheless, it is assumed to be sufficient to capture the in-plane strength relationship as fibres are aligned to best carry the applied tri-axial stresses, which is the case for maximum in-plane strength design in a Netting analysis regime [2,18]. Thus the performance of a laminate under a vector of loading can be shown by the single attribute of in-plane elastic energy. In the following sections, laminates are first optimised using the techniques presented with a Genetic Algorithm before designs are analysed and the data presented in plots revealing the potential benefits and drawbacks of new and current methodologies.

2. Minimum mass laminate design

In this section, a process is defined that minimises in-plane elastic energy under fixed and uncertain in-plane multi-axial loadings (axial, transverse, shear) in order to find distributions of SA and NSA plies that maximise laminate efficiency and thus minimise mass. Design constraints for both SA and NSA laminates, in the form of stacking sequence rules, are also derived.

2.1 In-plane elastic energy

Given that the in-plane Hookean or elastic energy for a linear elastic solid is

$$u = \frac{1}{2}\int \boldsymbol{\sigma}^{\boldsymbol{T}}\boldsymbol{\varepsilon}\, dV \tag{1}$$

Considering the in-plane laminate stiffness matrix, $\bar{\boldsymbol{Q}}$, the strain terms in Eq. (1), $\boldsymbol{\varepsilon}$, can be substituted for $\bar{\boldsymbol{Q}}^{-1}\boldsymbol{\sigma}$, allowing the elastic energy to be expressed using solely laminate level stresses, $\boldsymbol{\sigma}$. These stresses

(load per unit laminate cross-sectional area) can be further substituted with the equivalent in-plane loads per unit width, $\boldsymbol{N}$, divided by the laminate thickness, T.

$$u = \frac{1}{2}\int \frac{\boldsymbol{N}^T}{T}\bar{\boldsymbol{Q}}^{-\mathbf{1}}\frac{\boldsymbol{N}}{T}\,dV = \frac{1}{2}\int \boldsymbol{\sigma}^T\bar{\boldsymbol{Q}}^{-\mathbf{1}}\boldsymbol{\sigma}\,dV \tag{2}$$

Assuming a balanced laminate ($\bar{Q}_{16} = \bar{Q}_{26} = 0$) and working per unit volume allowing for laminate geometry to be ignored further implies

$$U = \frac{1}{2}\,\boldsymbol{\sigma}^T\bar{\boldsymbol{Q}}^{-\mathbf{1}}\boldsymbol{\sigma} = \frac{1}{2}\left(q_{11}\sigma_x^2 + 2q_{12}\sigma_x\sigma_y + q_{22}\sigma_y^2 + q_{66}\tau_{xy}^2\right) \tag{3}$$

where q terms are from the inverse of the laminate stiffness matrix. Division of Eq. (3) by the sum of the squares of the principal stresses normalises U, removing the effect of the magnitudes of the loads/stresses, and allows for an equal comparison between loading states of the same magnitude i.e.

$$\bar{U} = \frac{q_{11}\sigma_x^2 + 2q_{12}\sigma_x\sigma_y + q_{22}\sigma_y^2 + q_{66}\tau_{xy}^2}{2(\sigma_I^2 + \sigma_{II}^2)} \tag{4}$$

Where

$$\sigma_{I,II} = \frac{\sigma_x + \sigma_y}{2} \pm \sqrt{\left(\frac{\sigma_x - \sigma_y}{2}\right)^2 + \tau_{xy}^2} \tag{5}$$

The misalignment angle, η, of the principal loading from the balancing axes (about which $+\theta$ and $-\theta$ plies are evenly distributed to prevent extension shear coupling) is shown in Fig. 1 and defined as

$$\eta = \frac{1}{2}\tan^{-1}\left(\frac{2\tau_{xy}}{\sigma_x - \sigma_y}\right) \tag{6}$$

Substitution of Eq. (5) into Eq. (4) gives the expression for normalised elastic energy per unit volume, representing the effective laminate compliance that is independent of load magnitude and laminate thickness. A lower value corresponds to a higher global laminate stiffness, a more efficient use of material and thus a smaller amount of material required to support a certain load [18] i.e. minimum normalised elastic energy is equivalent to minimum mass.

$$\bar{U} = \frac{q_{11}\sigma_x^2 + 2q_{12}\sigma_x\sigma_y + q_{22}\sigma_y^2 + q_{66}\tau_{xy}^2}{2(\sigma_x^2 + \sigma_y^2 + 2\tau_{xy}^2)} \tag{7}$$

If the laminate is not balanced, either for all axes, or in the axes in which the elastic energy is calculated then $q_{16}\sigma_x\tau_{xy}$ and $q_{26}\sigma_y\tau_{xy}$ terms appear in the numerator of Eq. (7).

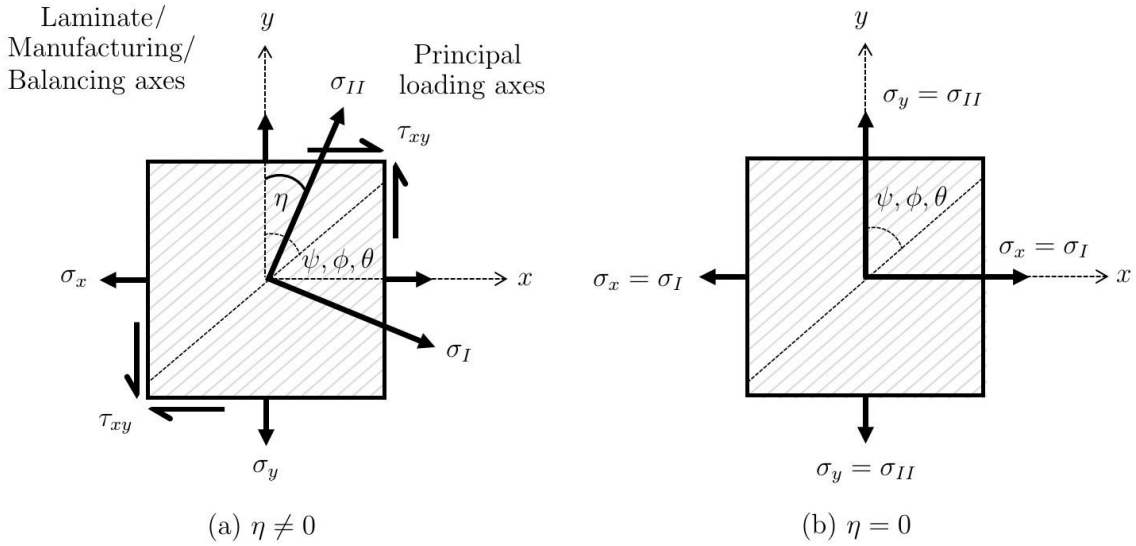

Figure 1. (a) Diagram showing laminate (*x*,*y*) axes (from which ply angles (ψ ,ϕ, θ) are defined and balanced) and principal loading axes offset from balancing axes by angle η. For (b) η = 0 and thus the balancing axes are aligned with the principal loading axes.

2.2 Optimisation

2.2.1 Problem Description

Current design techniques consider a fixed critical loading condition, relating to some worst case from various critical ultimate loads that could be applied to an aircraft structure. Any uncertainty in secondary loading is considered to be negated by enforcement of a 10% minimum ply percentage rule [2]. The new design strategy proposed here, optimises directly for maximum in-plane stiffness for a critical design load case ($\sigma = (\sigma_x, \sigma_y, \tau_{xy})$) in which secondary loadings are uncertain. For example, a primary load being defined by the largest stress in the *x*, *y* or *xy* directions, e.g. if $\sigma_x, \geq \sigma_y, \tau_{xy}$, the secondary loadings are then σ_y and τ_{xy}. To provide a comparison of the current and proposed design practices, laminates are optimised for minimum normalised elastic energy (minimum mass) under either a fixed loading (current practice with the 10% rule) or uncertain loading (proposed strategy). The two strategies are compared under a worst case loading (σ_{WC}, laminate dependent) derived from the envelope of loadings ($V_\sigma = \sigma_{10}$ or σ_{20}) created by a deviation in secondary loads of up to either ±10% or ±20% of the primary load, assumed to represent realistic variations in loading. This assumption is based on a critical loading having a primary loading component that remains relatively stable in magnitude with some variation in the less dominant loadings. Loading uncertainty data would be required to create a more realistic and tailored design, as the loading uncertainty will vary with different parts across an aircraft. Thus the assumed uncertainty considered is used only to discover potential benefits of the proposed methodologies.

2.2.2 Designing for an uncertain loading

Critical laminate design depends on the worst loading case that could be applied. Hence, the design concept is to achieve maximum performance under the worst case loading (σ_{WC}) taken from the loading envelope defined by ±10% or ±20% uncertainty (V_σ). The worst loading case, σ_{WC}, corresponds to the loading where a laminate has the maximum normalised elastic energy ($\max_{\sigma \in V_\sigma} \bar{U}$). However, this is dependent on the range of loadings and the laminate design, defined by ply angles θ and their proportions γ (see Section 2.2.3). By keeping the value of primary loading fixed (e.g. σ_x), a three dimensional surface for normalised elastic energy as a function of the two secondary loading variables (e.g. σ_y and τ_{xy}) described by Eq. (7) can be created for each individual laminate design, see Fig. 2 .

The Extreme Value Theorem [19] is used for two variables, which evaluates the maxima (critical points) of Eq. (7) (with fixed $\bar{\boldsymbol{Q}}$) by taking its derivatives both globally and on the boundaries of the allowed range of loading created by the uncertainty (V_σ), and setting them to zero. If no global critical points of maxima lie within the bounds then the maxima for consideration of worst case performance must lie on the boundary. These values of normalised elastic energy are compared to find the worst case loading (σ_{WC}) and its corresponding normalised elastic energy ($\max_{\sigma \in V_\sigma} \bar{U} = \bar{U}_{WC}$). The anti-optimisation problem is then summarised as finding the laminate design which minimises the worst case energy from the range of loads that could be applied from the uncertainty about a given design loading (see Eq. (8)).

$$\min_{\theta;\gamma} \left(\max_{\sigma \in V_\sigma} \bar{U} \right) \tag{8}$$

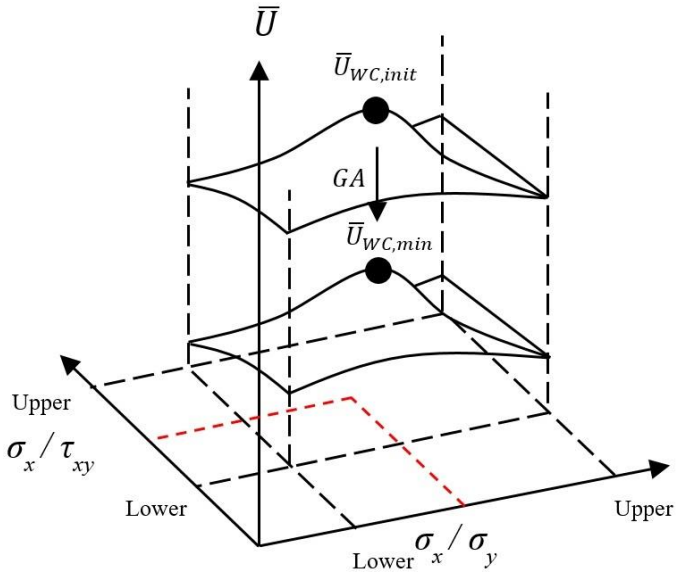

Figure 2. Schematic of optimisation for an uncertain design loading using a Genetic Algorithm in combination with the Extreme Value theorem to find optimal designs under worst case loading.

2.2.3 Optimisation strategies and variables

Laminates to be optimised contain either SAs or NSAs, and are designed using a MATLAB Genetic Algorithm (GA) 'ga' [20-23] for a fixed or an uncertain design loading (see Fig. 2 and Fig. 3(a) and (b)) as shown in Table 1. Laminated aerospace structures are, in general, subject to a combination of in-plane axial, transverse and shear load. As described in Section 2.1, optimal laminate designs will efficiently distribute fibres to meet these loads producing a laminate with minimum elastic energy.

SA designs are assumed to be balanced ($\bar{Q}_{16} = \bar{Q}_{26} = 0$) and symmetric ($B_{ij} = 0$, i, j = 1, 2, 6) and are described by two independent (γ_0 and γ_{45}) ply percentage variables. NSA designs are described by three integer angle variables (between 0-180°) and two independent ply percentage variables (γ_ψ and γ_ϕ), see Table 1. Each of the three main angles (ψ, ϕ, θ) within a NSA laminate is assumed to be made up of an infinite number of fully uncoupled blocks [24]. Each block [$+\theta/-\theta/-\theta/+\theta/-\theta/+\theta/+\theta/-\theta$] is divided in half about the laminate mid-plane creating anti-symmetry. These blocks ensure $\bar{Q}_{16} = \bar{Q}_{26} = B_{ij} = 0$ but are not a requirement as long as other stacking techniques can be used to maintain this condition. Note that variables are defined such that SA designs are a subset of NSA designs and so an SA design could be returned in an NSA optimisation run if it is the optimal laminate design. To reduce the computation required in the optimisation of designs to a manageable level, discrete ply stacking sequences are discarded in favour of continuous ply percentages. This has the advantage that all possible designs are assessed and a global picture of preferred design strategy is produced. However, there is a disadvantage in that some designs will not be discretisable into standard ply thicknesses (depending on total laminate thickness) and thus results will be inconclusive for load cases where competing design strategies produce laminates with little difference in performance.

Design strategy ID	Angles (integer °)	Ply %'s	Design Load	10% Rule	Ply Unblocking Rule
SA1	0, ±45, 90	γ_0, γ_{45}, 1- (γ_0 + γ_{45})	Fixed	✓	✓
NSA1	$\pm\psi$, $\pm\phi$, $\pm\theta$	γ_ψ, γ_ϕ, 1- (γ_ψ + γ_ϕ)	Fixed	×	✓
SA2	0, ±45, 90	γ_0, γ_{45}, 1- (γ_0 + γ_{45})	Uncertain	×	✓
NSA2	$\pm\psi$, $\pm\phi$, $\pm\theta$	γ_ψ, γ_ϕ, 1- (γ_ψ + γ_ϕ)	Uncertain	×	✓

Table 1. Details of four design strategies considered in the laminate design optimisation, angle variables, ply percentages variables and active design rules. γ_{45}, γ_ϕ and γ_ψ are the total proportions for angles of ±45, $\pm\psi$ and $\pm\phi$, respectively.

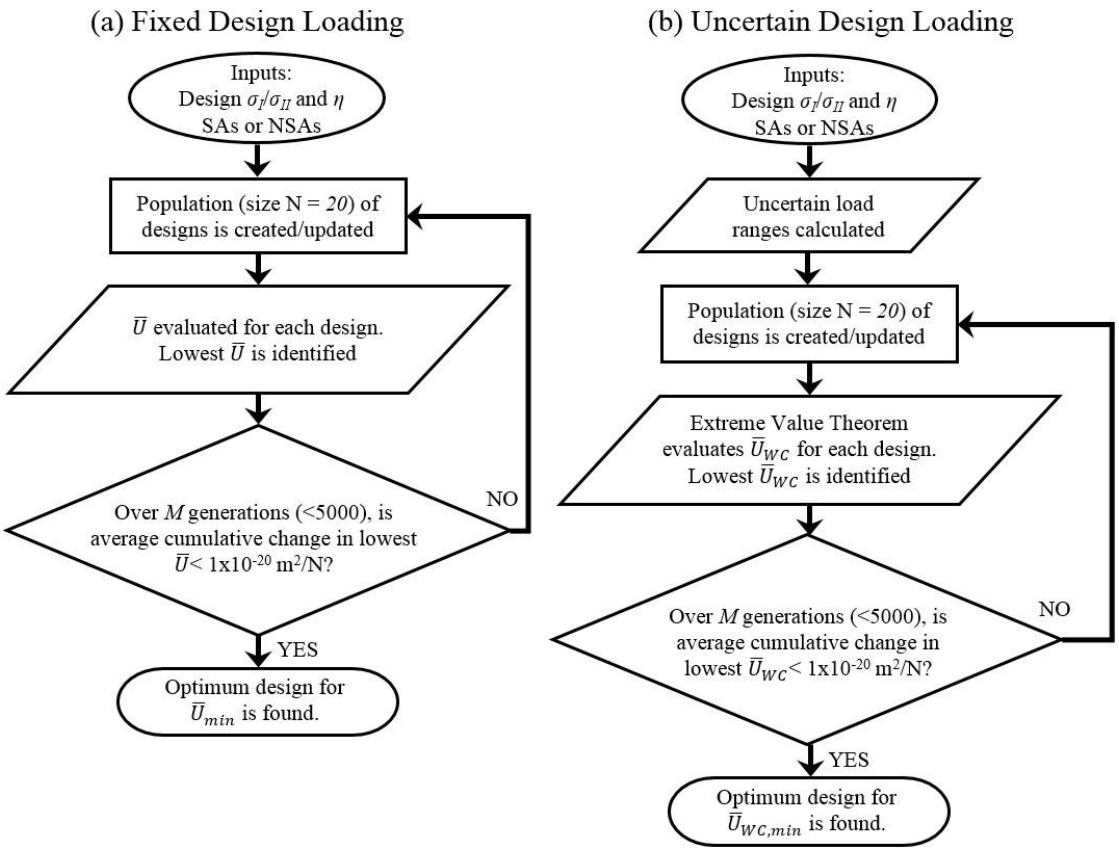

Figure 3. Optimisation procedure for design of a laminate for minimum elastic energy under (a) a fixed design loading and (b) an uncertain design loading.

2.2.4 Laminate design rules

Design rules are applied in laminate design in order to account for non-design failure mechanisms and to ensure favourable deformation which may not be taken care of during the design optimisation [2]. The two extra design rules, in addition to the balancing requirement of $\bar{Q}_{16} = \bar{Q}_{26} = B_{ij} = 0$, are:

1) Ply unblocking: To prevent the formation of large inter-laminar shear stresses that may drive free edge failure, and thermal stresses that could cause premature failure, a maximum of four contiguous plies of the same/similar orientation is allowed [2]. In SA designs, compliance is ensured by requiring that the ply percentages of the non-dominant perpendicular plies (either 0° or 90°) added to that of the ±45° plies, sum to at least one quarter of the dominant 0° or 90° ply percentage, i.e. for every four dominant plies there is one ply that differs by at least 45° (4:1). In NSA designs, ply groups of similar angles are assumed to be unblocked by an angular separation of at least 22.5°. The GA can choose between two techniques to find an optimal design:

(i) Use of higher angles ($|\pm\theta| \geq 22.5°$) to unblock dominant lower angles ($|\pm\theta| < 22.5°$) and vice versa ($|\pm\theta| \leq 67.5°$ unblock $|\pm\theta| > 67.5°$). Similarly to SAs, a 4:1 ratio of dominant and

non-dominant ply angles is maintained. The angles used to unblock are assumed to be placed in a fashion that is symmetric and balanced, maintaining $\bar{Q}_{16} = \bar{Q}_{26} = B_{ij} = 0$.

(ii) Where ply percentages of the two non-dominant angles are too low to meet unblocking requirements in (i), all plies with $|\pm\theta| < 22.5°$ or $> 67.5°$ associated with the maximum ply percentage are swapped for ±22.5° or ±67.5° as appropriate.

2) 10% minimum ply percentage: In current SA laminate design practice, a 10% minimum of each of 0º, 45º, -45º and 90º ply angles safeguards against uncertainty in loading (SA1, Table 1). This rule is enforced for SA1 designs by limiting the choice of ply percentages available to the GA. No convention for enforcing this rule on NSA designs exists. Instead, here, the optimisation procedure in Section 2.2.6 designs directly for uncertainty in loading. This procedure is applied in both SA and NSA design strategies, see SA2 and NSA2 in Table 1.

2.2.5 Design Loading and Principal Loading Misalignment

SA laminates are normally restricted to a fixed 'manufacturing' (*x,y)* coordinate system about which laminates are balanced (for example, 0° fibres are aligned from root to tip in a wing skin) [2]. In both SA and NSA laminates, an equal number of positive and negative angle plies ensures designs are balanced about the (*x,y)* axes, see Fig. 1. All general load states can be described by their principal loading and a misalignment angle, η, from the (*x,y)* balancing axes, see Fig. 1. For example, $\eta = \pi/4$ indicates a state of pure shear is applied in the balancing axes. $\eta = 0$ is also a special case where the principal loading axes are aligned with the balancing axes, see Fig. 1(b). This is generally not the case in design as balancing axes are usually aligned with the laminate manufacturing axes. However, balance can theoretically be achieved in axes other than the manufacturing axes, such as the principal axes, thereby achieving $\eta = 0$. In the results that follow 257 principal loading ratios, σ_I/σ_{II} (from ∞ to $-\infty$), and 513 principal axes misalignments, η (from $\pi/2$ to $-\pi/2$), are considered creating 131,841 different design loading scenarios.

A designer with a given design loading in the laminate axes (*x,y*), described by the ratios between, or magnitudes of, the three stresses σ_x, σ_y and τ_{xy}, can, using Eq.(5) and Eq.(6) respectively, convert this loading into the principal loading ratio σ_I/σ_{II} and misalignment angle η. To convert any (*x,y*) design load or ratio into a principal design load (and a value of η) arbitrary values of (*x,y*) stress in the correct ratio (the absolute values are irrelevant) should be input into Eqs. (5) and (6) and the quotient of the result taken to produce σ_I/σ_{II}.

When considering the results that follow in Section 3, it may help the reader to know the desi gn loading in the laminate axes (x,y) for a given σ_I/σ_{II} and η, as these latter variables form the plot axes. (x,y) stresses can be determined using Eqs. (9-11) with arbitrary values of σ_I and σ_{II} in the correct ratio.

$$\sigma_x = \frac{\sigma_I + \sigma_{II}}{2} + \frac{\sigma_I - \sigma_{II}}{2}\cos 2\eta \tag{9}$$

$$\sigma_y = \frac{\sigma_I + \sigma_{II}}{2} - \frac{\sigma_I - \sigma_{II}}{2}\cos 2\eta \tag{10}$$

$$\tau_{xy} = -\frac{\sigma_I - \sigma_{II}}{2}\sin 2\eta \tag{11}$$

2.2.6 Optimisation using Genetic Algorithm

A MATLAB GA is implemented which optimises either (i) two ply proportions or (ii) two ply proportions and three ply angle variables, describing the SA and NSA designs (see Table 1) respectively, to produce minimum normalised elastic energy under multiple fixed ($\overline{U}_{min}$) and uncertain ($\overline{U}_{WC,min}$, see Fig. 2) tri-axial design loadings (σ_I/σ_{II} and η). The default GA settings are used unless otherwise stated [20]. Lower and upper bounds are set on the GA input variables at 0-90° for the NSA angles and 0-1 (0-100%) for the ply proportions (percentages). IntCon is used for the NSA optimisations to ensure that all 3 angles are integers. Full details of how the GA works are given here [20], a brief summary of the process follows. GA creates an initial random population (of size N = 20) of candidate design variables and calculates a scored fitness value for each. The lowest energy designs are chosen and used to determine the next generation/population of design variables. Eliteness, crossover and mutation all feature in '*ga'*. The Elite count is set at 5% of the Population size. A Crossover fraction of 0.8 was used. The Mutation function is only employed for SA optimisations whereby a Gaussian mutation is used with Scale and Shrink both equal to 1. Integer constraints on the NSA optimisation prevent Mutation from being implemented. Iteration continues until the stopping criteria of a maximum number of iterations reaches 5000 or if the change in the normalised elastic energy value between iterations is less than $1\text{x}10^{-20}$ m^2/N, (Note that none of the results below were derived as a consequence of the maximum number of iterations limit being reached).

2.2.7 Mass equivalence to minimum elastic energy

Assuming a magnitude of u (see, Eq.(2)) that causes failure throughout the laminate, u_{fail}, and an ultimate loading, $\boldsymbol{N}_{ult}$, that must be carried, the laminate stiffness, $\overline{\boldsymbol{Q}}$, and thickness, T, can be varied to ensure failure does not occur before this ultimate loading by ensuring $u \leq u_{fail}$, see Eq. (12)

$$u = \frac{1}{2T^2} \boldsymbol{N}_{ult}^{T} \bar{\boldsymbol{Q}}^{-1} \boldsymbol{N}_{ult} \tag{12}$$

If failure occurs at this ultimate loading, then a laminate has the minimum amount of thickness and thus mass required to carry this loading. Note that this assumes failure is not being considered at the ply level.

$$u_{fail} = \frac{1}{2T_{min}^2} \boldsymbol{N}_{ult}^{T} \bar{\boldsymbol{Q}}^{-1} \boldsymbol{N}_{ult} \tag{13}$$

It then follows that $T_{min}^2 \propto \bar{\boldsymbol{Q}}^{-1}$ and $T_{min} \propto \sqrt{\bar{\boldsymbol{Q}}^{-1}}$. Thus the thickness of the laminate depends on the optimality of $\bar{\boldsymbol{Q}}^{-1}$ and as $\bar{U} \propto \bar{\boldsymbol{Q}}^{-1}$ then the laminate mass $\propto \sqrt{\bar{U}}$. Designs in this paper are optimised for minimum $\bar{U}$ but do not have a thickness/mass**.** However designs would be minimum mass if thickness is tailored to the correct failure value and ultimate load magnitude. There is no specific value of u_{ult} that corresponds to failure strength predictions and so laminate mass determination is not possible for a given magnitude of ultimate loading, $\boldsymbol{N}_{ult}$. Despite this, mass savings of one design technique over another can be calculated by comparing the values of $\sqrt{\bar{U}}$. The laminate energy, u, cannot be used to predict failure as it does not account for all realistic failure mechanisms on the mirco, meso and macro levels. It can only be used as a proxy for strength, thus $\bar{U}$ is used as a performance marker only, where the ability to rank designs is thought to be sufficient to find a suitable optimum design.

3. Results

In the results that follow material properties of E_{11} = 128 GPa, E_{22} = 10 GPa, G_{12} = 4.5 GPa, ν_{12} = 0.3 for AS4/8552 are assumed. General design loadings (σ_x, σ_y and τ_{xy}) are represented by the ratio of principal stresses, σ_I/σ_{II}, and the misalignment of principal loading axes from the balancing axes, η, (established from σ_x, σ_y and τ_{xy} via Mohr's Circle, see Eqs. (5) and (6)). However, initially in Figs. 4 and 5, to aid the reader in understanding the results, η is given two fixed values (0 and π/8 rad) with later results showing a continuous variation in η. In Figs. 4-9 the principal load ratio, σ_I/σ_{II} = 1, indicates hydrostatic loading for all η. For a ratio of σ_I/σ_{II} = -1 pure shear exists at a misalignment of the principal axes of $\eta = \pm(2n\text{-}1)\pi/4$, where n = 1,2,3…∞. For example in Fig. 4(a), when η = 0 and σ_I/σ_{II} = -1, SA optimum designs with the 10% rule occur that have ply percentages 40/20/40 (% of 0°/±45°/90°). It is noted, such designs give SA ply percentages in the pure shear axis at $\eta = \pi/4$ (45°) that are typical for a spar i.e. 10/80/10.

Figures 4(a) and (b) show ply percentages for optimum SA designs under fixed loading i.e. 0% uncertainty. Similarly, Figs. 4(c) and (d) show optimum designs related to the NSA1 design technique. Figures 4(e) and (f) demonstrate the effect of design rules using SAs or NSAs on the normalised elastic

energy of optimised laminates under their design loadings including the energy of designs presented in Figs. 4(a-d). Low energy is indicative of more efficient use of material.

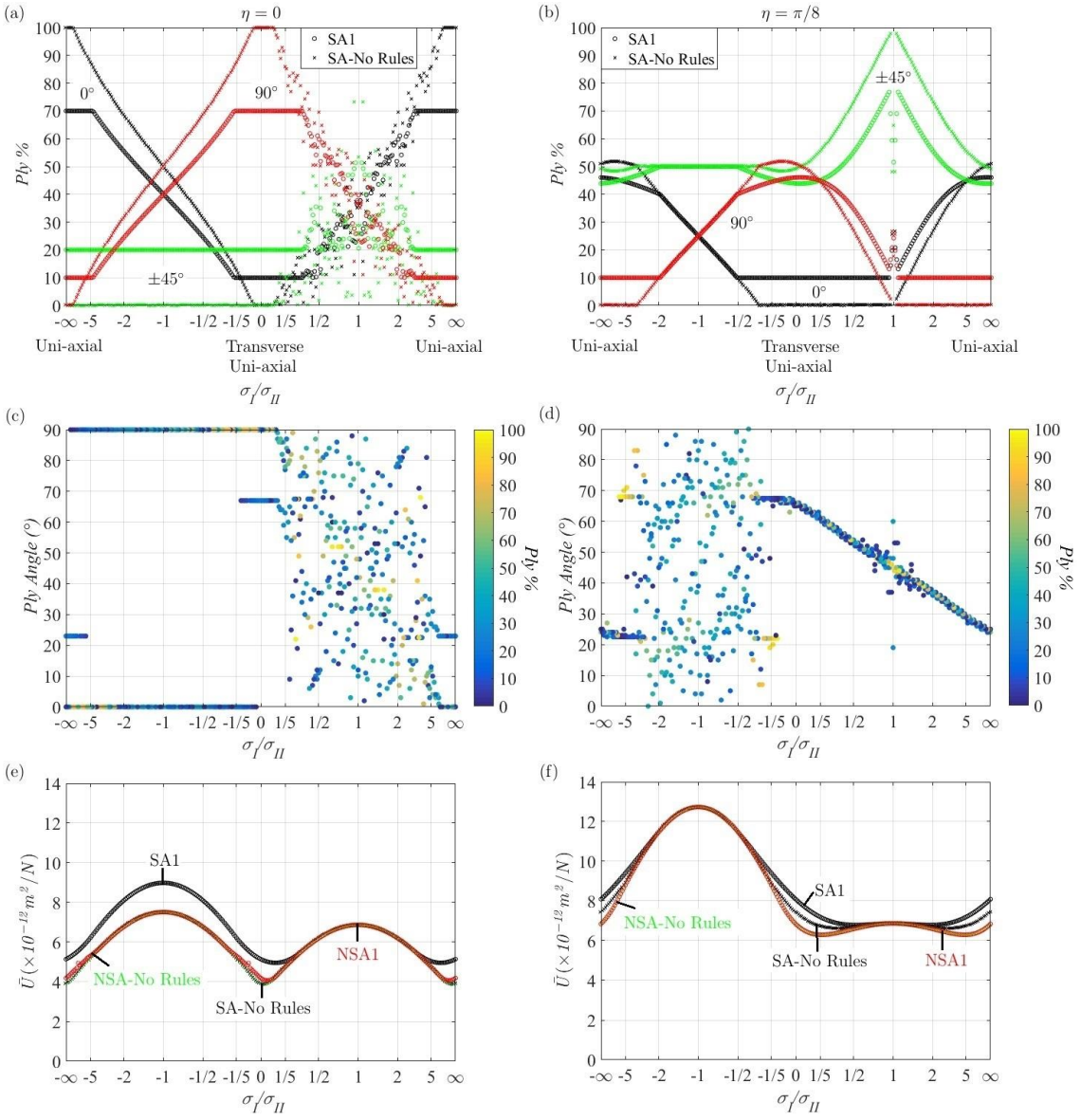

Figure 4. SA ply percentages for optimum minimum elastic energy designs under a fixed loading are given for (a) $\eta = 0$ and (b) $\eta = \pi/8$. Cross (circle) markers indicate unconstrained (constrained SA1) laminates. NSA ply angles and percentages for optimum NSA1 designs are given for (c) $\eta = 0$ and (d) $\eta = \pi/8$. Normalised elastic energy of minimum elastic energy laminates, $\bar{U}$, with standard and non-standard ply angles for loadings with (e) $\eta = 0$ and (f) $\eta = \pi/8$.

Figures 5 (a), (b), (c) and (d), show, respectively, the normalised elastic energies of optimised laminates, for each of the four design strategies SA1, NSA1, SA2 and NSA2 (see Table 1), under a worst case loading applied within the range of loading uncertainty that exists for each design loading (±10% or ±20%).

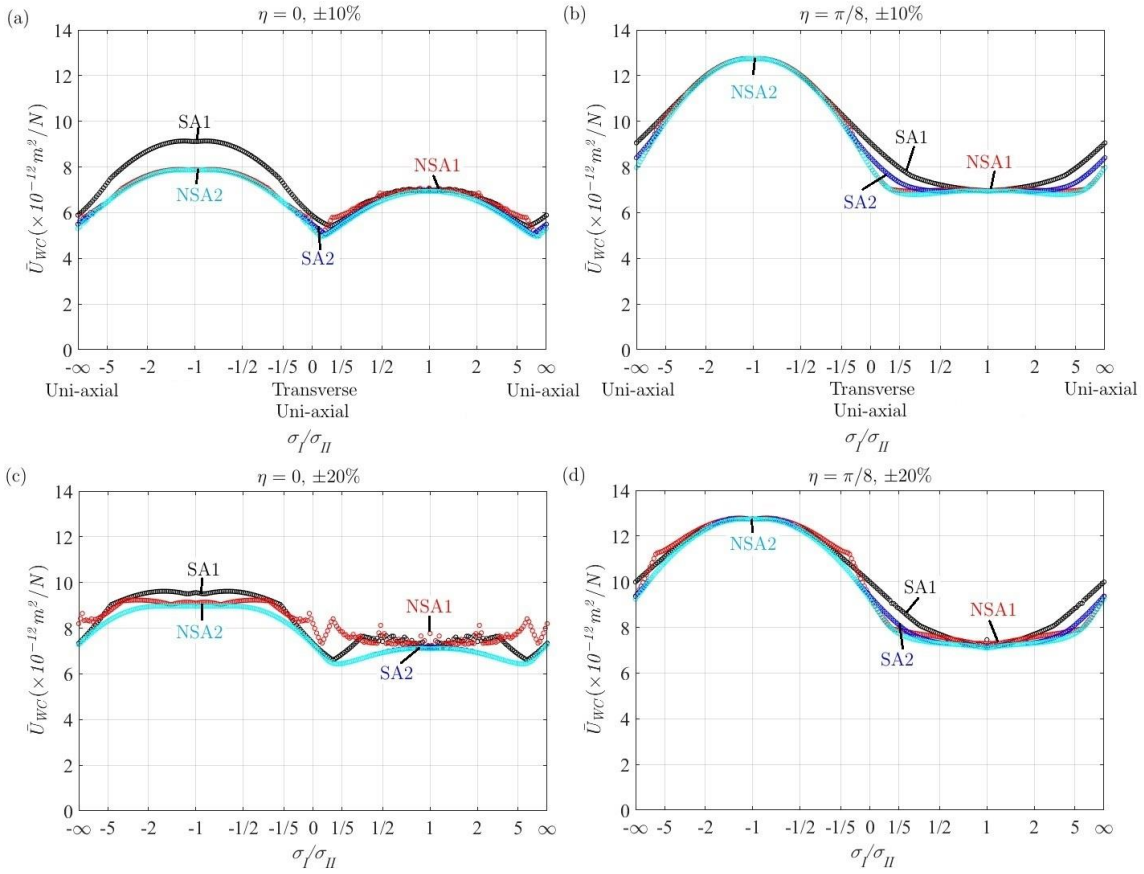

Figure 5. (a-d) variation in worst case normalised elastic energy, $\bar{U}_{WC}$ designs subject to ±10%, (a-b) or ±20%, (c-d) uncertainty in design load (see Section 2.2) for η = 0 or $\pi/8$.

In Figs. 6(a)-(d), η is allowed to vary continuously. Individual points represent an optimised laminate design and are coloured according to the normalised elastic energy produced when the worst case loading derived from an uncertainty of ±10% is applied. Figures 6(a), (b), (c) and (d) provide results for design strategies SA1, NSA1, SA2 and NSA2 (see Table 1) respectively.

Figure 7 shows ply angles and ply percentages for optimum laminate designs derived from the SA1 (current practice) and NSA2 (strategy with greatest potential) design strategies under the worst case loadings seen in Figs. 6(a) and (d) respectively. Angle variables for NSA2 designs are ordered such that the lowest magnitude of angle (e.g. 0°) is associated with the uppermost plots Fig. 7 (d) and (g), and the highest (e.g. 90°) with the lowermost plots Fig. 7 (f) and (i). Figure 7 is not designed to enable identification of individual designs but instead to indicate the make-up of designs in regions of similar loading scenarios. For example, for η = 0, $\sigma_I/\sigma_{II} \approx 0$ i.e. dominant σ_{II}, Fig. 7 (d), (e), (g) and (h) show very low % of low angle plies with Fig. 7 (c) and Figs. 7 (f) and (i) showing very high % of 90° plies. In contrast near $\eta = -\pi/8$, σ_I/σ_{II} = -1, loading is more balanced in σ_I, σ_{II} and has a significant τ_{xy} component in the manufacturing axes. This leads to designs with roughly equal percentages of low, medium and high

angles or 0°, ±45°, 90° plies for NSA and SA respectively. Where an even distribution of ply angles is required, multiple solutions exist and the design space becomes fuzzy.

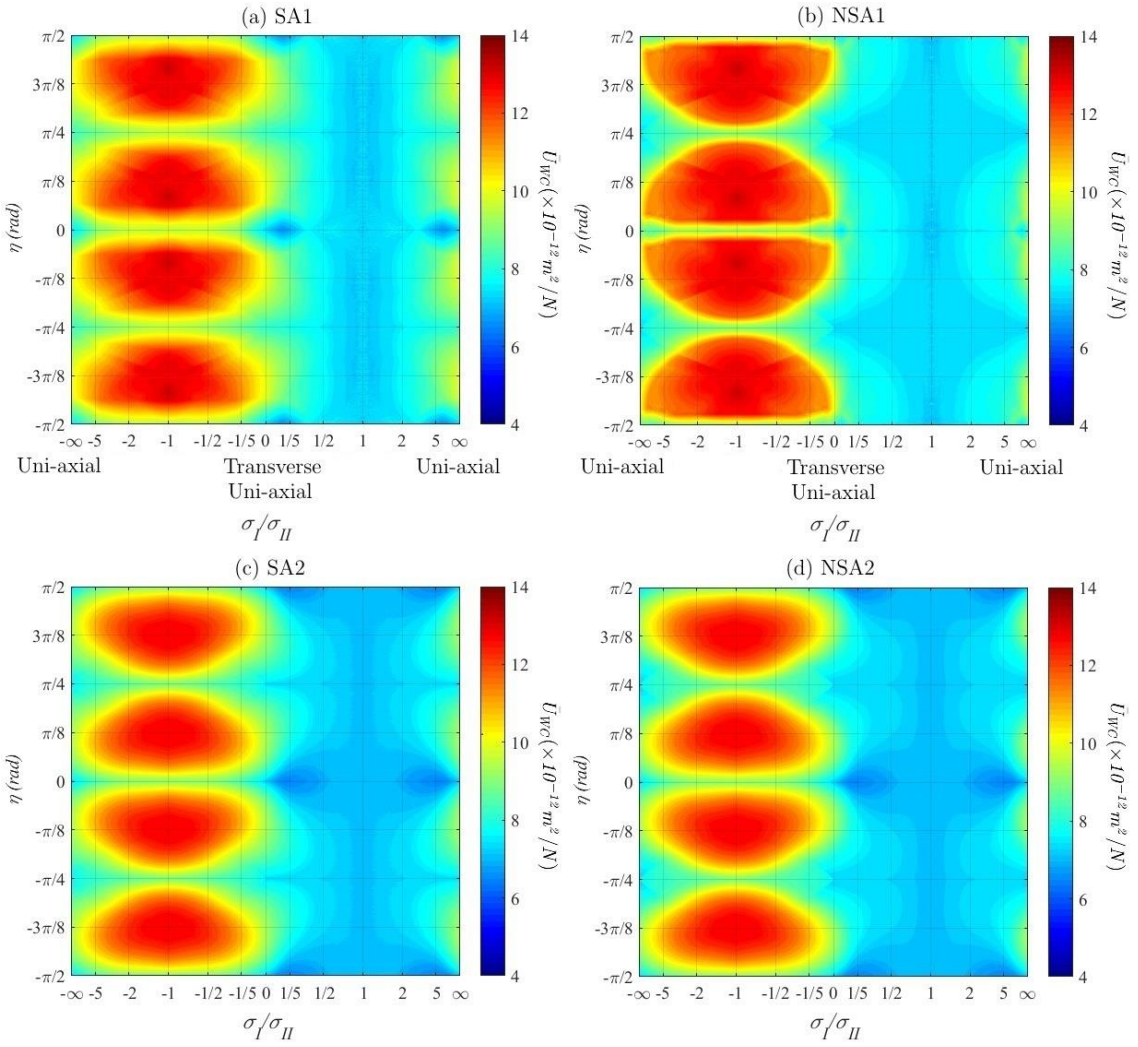

Figure 6. Laminate normalised elastic energies (Eq. (8)) under worst case loading for a range of general design loadings described by σ_I/σ_{II} and η with ±20% uncertainty. (a) SA1: 10% minimum ply percentage rule accounts for load uncertainty. (b) NSA1: no load uncertainty considered. (c) SA2: no 10% rule, designed directly for load uncertainty. (d) NSA2: designed directly for load uncertainty.

Figure 8 shows mass saving plots illustrating differences in $\sqrt{\bar{U}_{WC}}$ (see Section 2.2.7) for different design strategies. Plots are derived for both ±10% and ±20% uncertainty by subtraction of values for one design strategy from another. SA2 is compared to SA1, NSA2 to SA1 and NSA2 to SA2 shown in Figs. 8(a-b), (c-d) and (e-f), respectively.

Figure 9 is constructed by plotting the percentage difference between maximum and minimum values for $\sqrt{\bar{U}_{WC}}$ that fall on any vertical line in Fig. 6(a). Minimum $\sqrt{\bar{U}_{WC}}$ occurs for η = 0 and maximum values occur for some worst case value of η. Thus Fig. 9 indicates maximum mass savings that can be obtained for an SA1 and NSA2 design strategy if, in a notional design problem, balancing axes were realigned from some worst case alignment to the principle loading axes.

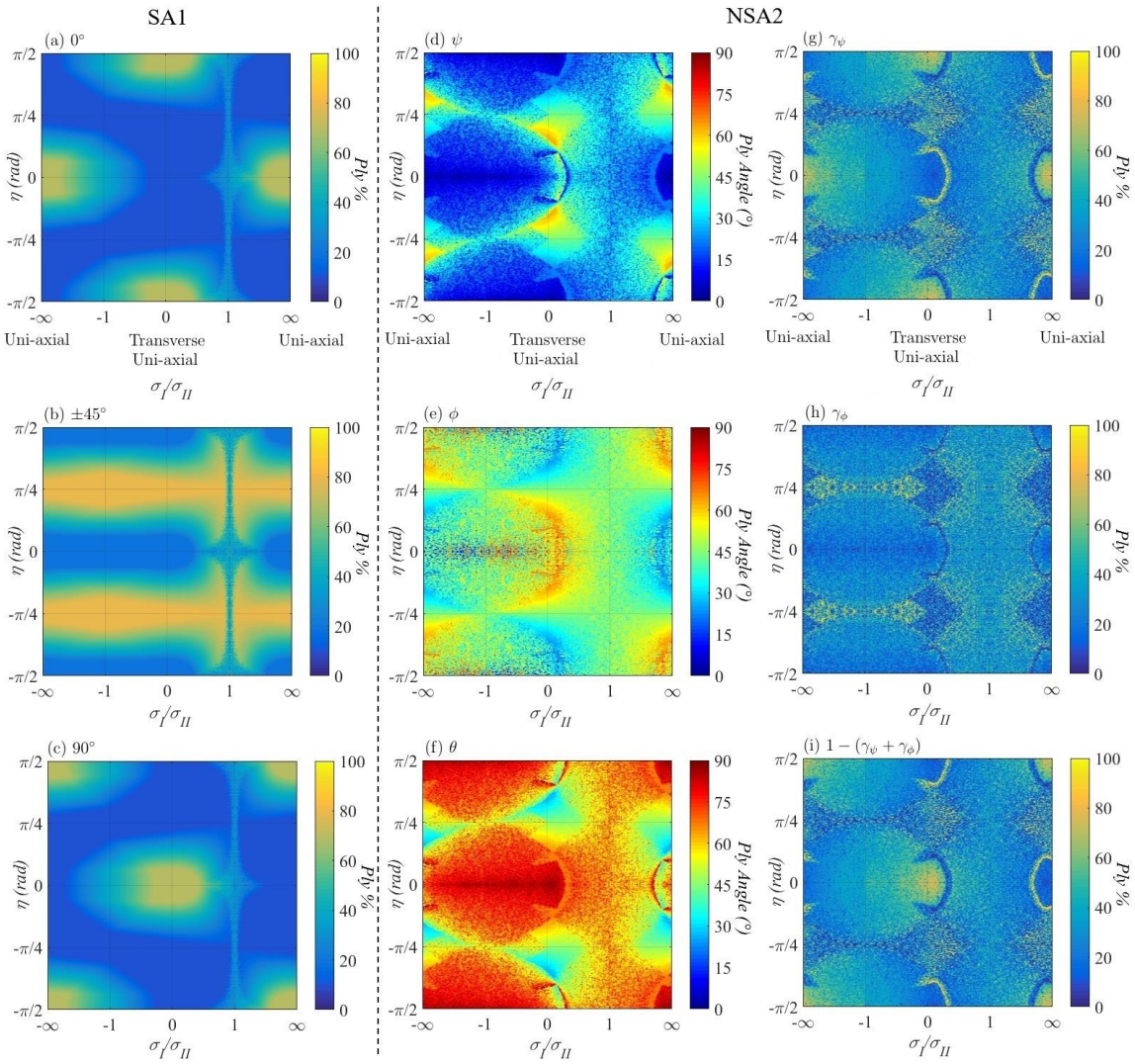

Figure 7. Percentages of (a) 0°, (b) ±45° and (c) 90° plies in SA1 designs of Figure 6(a) where a 10% minimum ply percentage rule accounts for load uncertainty. Ply angles lowest to highest (d-f) and related ply percentages (g-i) respectively for NSA2 designs of Figure 6(d) where ±20% uncertainty in loading is designed for, see Section 2.2.

4. Discussion

It is noted that the approach of equating minimum in-plane energy with improved performance/minimum mass is only applicable to laminates that fail via in-plane fibre based mechanisms. No attempt is made to account for damaged based failures or structural failures such as buckling. Furthermore, designs presented are formed from continuous ply percentages and thus results are more representative of thick laminates (or those made with thin plies) where ratios of ply percentages are more achievable. This is compounded for NSA designs which rely on an entirely uncoupled laminate structure [24] that might constrain the design space.

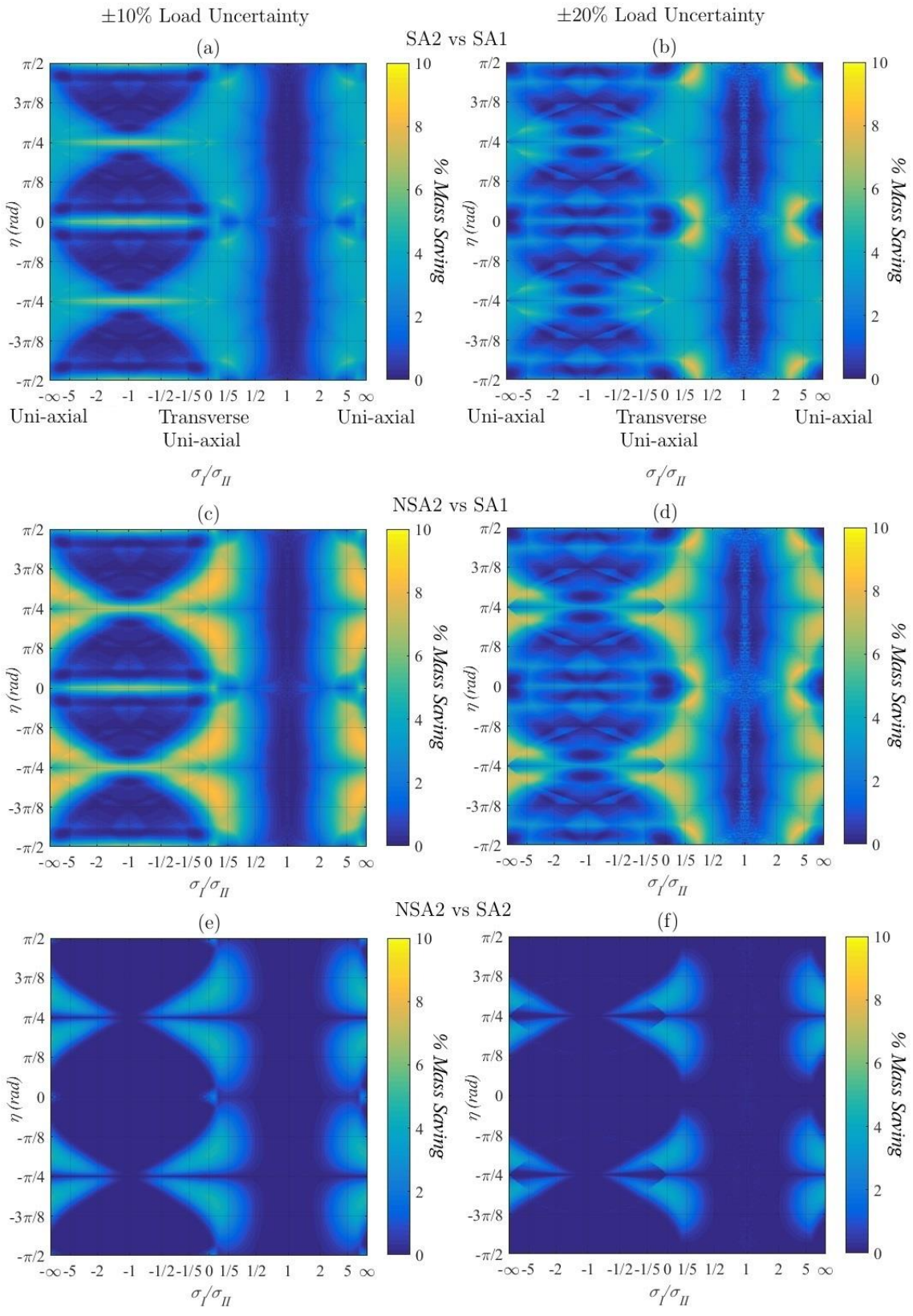

Figure 8. Mass savings derived from different design strategies for variable η and design loadings described by σ_I/σ_{II} with an uncertainty of ±10% or ±20% left and right hand plots respectively. (a) and (b) percentage mass saving of an SA2 strategy over an SA1 strategy, (c) and (d) percentage mass saving for an NSA2 strategy over an SA1 strategy. (e) and (f) percentage mass saving for an NSA2 strategy over an SA2 strategy.

4.1 Energy extrema and the effect of misalignment of balancing and principal loading axes

Single axis loading and thus single axis optimal fibre orientations create energy minima, e.g. at $\sigma_I/\sigma_{II} \approx 0$ and ∞ in Fig. 4(e). Minimum energy for all load ratios in Fig. 6 lies on lines of $\eta = 0 \pm n\pi/2$. This indicates that laminate design can be improved significantly by balancing laminates in the principal loading axes. Indeed, in Fig. 9 a maximum mass saving of 20% is possible at $\sigma_I/\sigma_{II} = 10.15$ or 0.99 when using the current, SA1, design practice and balancing laminates in the principal loading axes. As the variation in energy with η across the loadings in Fig. 6 is nonlinear, the realistic mass saving from employing this technique will be highly dependent on the original misalignment η, the σ_I/σ_{II} design load ratio and the uncertainty in loading considered. For example, near $\sigma_I/\sigma_{II} = 1$ the energy shows little variation with η in comparison to those near $\sigma_I/\sigma_{II} = -1$, see also Fig. 9. Previous work has shown the effect of principal load ratio on potential mass saving when balancing about the principal loading axes [25]. Mass savings of up to 22% are possible when employing this technique when designing directly for the uncertainty using NSAs ($\sigma_I/\sigma_{II} = -1$).

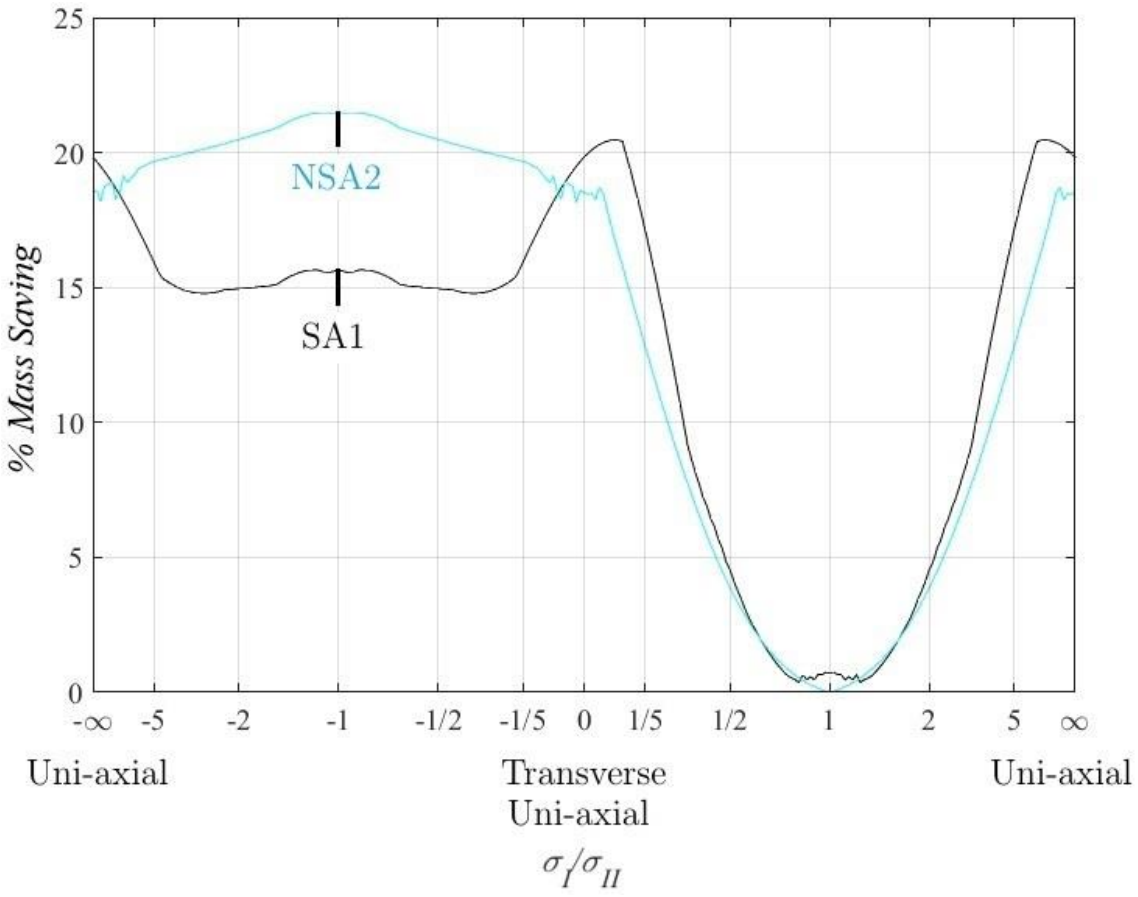

Fig. 9. Mass saving from balancing laminates in the principal loading axes, $\eta = 0$, compared to balancing at the worst misalignment from the range of possible η for all σ_I/σ_{II} design loadings ratios using the SA1 and the NSA2 strategies when a loading uncertainty of ±10% is applied.

Energy maxima or high mass designs for $\eta = 0$ (Fig. 4 (e)) occur where orthogonal principal stresses with equal magnitude ($\sigma_I/\sigma_{II} \approx 1$ and $\sigma_I/\sigma_{II} \approx -1$) create the greatest difference in requirements for optimal stiffness. Indeed, Fig. 6 indicates that maxima continue to occur at $\sigma_I/\sigma_{II} \approx 1$ for any fixed η.

As is evident in Figs. 4 and 6, maxima in the vicinity of $\sigma_I/\sigma_{II} = -1$ are larger than $\sigma_I/\sigma_{II} = 1$. This is a consequence of the sign of $2q_{12}\sigma_I\sigma_{II}$ in Eq. (7). The value of $2q_{12}\sigma_I\sigma_{II}$ is positive for $\sigma_I/\sigma_{II} < 0$ and thus is additive to the energy stored. Physically this is due to the softer laminate response to the compression-tension loading acting in the same direction as the laminate Poisson's ratio deformation. Conversely for $\sigma_I/\sigma_{II} > 0$, the $2q_{12}\sigma_I\sigma_{II}$ term is negative resulting in lower energies and a stiffer laminate response due to loading acting against Poisson's ratio deformation.

Comparison of Figs. 4(e) and (f) shows that an increase in η from 0 to $\pi/8$ increases energy for all σ_I/σ_{II} ratios with the exception of hydrostatic ratios. For hydrostatic ratios alignment of principal load has no effect on loading present in the laminate axes due to equal loads being present in all directions. This increase is also seen in Fig. 6 as $\eta \rightarrow \pi/8$, and is a consequence of the $q_{66}\tau_{xy}$ term in Eq. (7) becoming non-zero with the introduction of a shear load component. Global maxima occur at $\eta = \pi/8, 3\pi/8$ where all design loads are the same magnitude and the axial and transverse loads have opposite sign ($\sigma_x = -\sigma_y = \tau_{xy}$). For these load ratios, design traits required to efficiently carry the three load components are in greatest conflict.

4.2 Minimum Energy design strategies and non-uniqueness of designs

Comparison of ply angles derived under ±10% loading uncertainty, using SA1 (Fig. 7(a)-(c)) and NSA2 (Fig. 7(d)-(i)) strategies indicate, irrespective of design strategy, 0°, 90°, ±45° plies dominate if the loading is axially, transverse or shear dominated, respectively. For example, for $\sigma_I/\sigma_{II} = 0$ and $\eta = 0$ in Fig. 7(c), (f) and (i) laminates with high proportions of 90° plies are optimal. Similarly, a comparison of Figs. 4(a) and (c) shows 0° and 90° plies are optimal in both SA and NSA designs when $\sigma_I/\sigma_{II} < 0$ and $\eta = 0$. This is a consequence of (i) a positive $2q_{12}\sigma_I\sigma_{II}$ term in Eq. (7) penalising the use of other angles with higher Poisson's ratios (which produce large negative q_{12} terms) and (ii) 0° and 90° plies minimising the energy storage associated with a softer laminate response. In Fig. 4(c) and (d), regions where straight horizontal lines appear at angles of 22.5° and 67.5° indicate the ply unblocking rule from Section 2.2.4 has prevented laminates from having too high a proportion of low ($|\pm\theta| < 22.5°$) or high ($|\pm\theta| > 67.5°$) angles that are employed by minimum energy designs. When $\sigma_I/\sigma_{II} < 0$ plots in Figure 7 show that as η tends from 0 to $\pi/4$, and thus loading in the balancing axes moves from purely bi-axial to combined bi-

axial and shear, optimum plies transition from purely 0° and 90° to mostly ±45° for both SA and NSA designs.

In contrast to the above, for $\sigma_I/\sigma_{II} > 0$ in Fig. 4 (a) and (c) and $\eta = 0$ in Fig. 7(d-i), the optimality of designs with ±45° and $\pm\theta$ angles can be seen. The Poisson's ratio increases brought about by these ply angles result in larger negative q_{12} and act to increase the effective laminate stiffness for $\sigma_I/\sigma_{II} > 0$ thereby decreasing the energy stored. This is not true when $\eta = \pi/8$ near $\sigma_I/\sigma_{II} = 0$ and ∞ in Fig. 4(f). Here $q_{66}\tau_{xy} \neq 0$ in Eq. (7), as shear appears in the design loading, and optimal laminate stiffnesses are achieved by NSAs but not SAs which can only seek to minimise energy with non-optimal ±45° angles (contrast Figs. 4(b) and (d)). For example, ±30° and ±60° designs seen in Fig. 4(d) produce laminate stiffnesses that are unachievable by SAs in Figs. 4(b) [26].

Regions of scattered points in Figs. 4(a) and (c) for $\sigma_I/\sigma_{II} > 0$ and Fig 4(d) for $\sigma_I/\sigma_{II} < 0$, are a consequence of non-uniqueness of optimum laminate designs. Similarly, regions where colouring is 'noisy' in Figs 7(d)-(i) are also a result of non-uniqueness. For for $\sigma_I/\sigma_{II} > 0$ in Figs. 4(a) and (c) this is a consequence of a negative $2q_{12}\sigma_I\sigma_{II}$ term in Eq. (7). This negative term allows minimum energies to be met via different stiffness designs that either increase q_{12}, or decrease q_{11} and q_{22} (or a combination of the two). This implies for $\sigma_I/\sigma_{II} > 0$, different optimal $\overline{\boldsymbol{Q}}$ matrices exist for the same design loading and minimum $\overline{U}$. For $\sigma_I/\sigma_{II} < 0$ in Fig. 4(d) the $2q_{12}\sigma_I\sigma_{II}$ term in Eq. (7) must be positive and thus non-uniqueness in designs instead occurs as a consequence of the capacity of NSAs to provide multiple optimal solutions. Work in [25] shows that the stiffness of non 0° or non 90° plies can be matched by multiple bi-angle ply pairs thus indicating non-uniqueness. If all three angles ψ, ϕ and θ plies have angles other than 0° and 90° additional redundancy and hence non-uniqueness is introduced. Figs. 7(d), (e) and (f) show that designs for $\eta \neq 0 + n\pi/2$ are made up of plies other than 0° and 90° and thus designs are non-unique for the same reason. Non-uniqueness indicates that significant regions of the NSA loading space have multiple optimum solutions and thus offer a less constrained design space than the SA designs. This gives scope for optimising NSA solutions for a different purpose whilst maintaining the optimal laminate stiffness, potentially presenting an advantage over SA solutions.

4.3 Industrial design rules versus designing for uncertainty

Contrasting Figs. 5(c) and (d) with 5(a) and (b) shows that absolute values of energies for all design techniques increase with a ±20% load uncertainty as the potential applied loads can be more severe.

Comparison of plots in Figs. 5 and 8 shows that reductions in energy/mass when designing directly for uncertainty are smaller for 20% loading uncertainty than for 10% uncertainty. This implies that, although there is a greater uncertainty in loading, there is less of an advantage (depending on the value of η) in designing directly for this uncertainty.

Both the 10% rule and ply unblocking rule are detrimental to optimum designs under many load scenarios and comparison of plots in Figs 4(e) and (f) shows that design rules have a stronger effect for SAs than for NSAs. This is both a consequence of the fact that ±22.5° and ±67.5° plies are available for unblocking in NSA designs (compared to only ±45° in SA designs) which allows for better alignment of fibre and loading axes but mainly due to the fact that the 10% rule is not applied to NSAs. This ensures ≥ 30% of the angles in SA designs are non-dominant i.e. at least 10% of 0° and 90° and 20% of ±45° plies. The effect of design rules is most apparent when either loading is dominated by one component, and thus where plies of a single angle (0° or 90°) are optimal (e.g. $\sigma_I/\sigma_{II} \approx 0, \infty$, for $\eta = 0$) or where designs are prevented from reaching the more optimal 0% of ±45° unconstrained solutions (e.g. $\sigma_I/\sigma_{II} < 0$, $\eta = 0$) see Figs 4(a) and (e) and Fig. 5(a). Figure 8 (a) shows that for 10% uncertainty designing directly for an uncertain loading using standard angles (SA2) instead of using the 10% rule (SA1) creates a mass saving > 5% for only 3.0% of design loadings. This rises to 4.9% of design loadings when a ±20% loading uncertainty is considered with a peak mass saving of 8.2%, see Fig. 8(b). A greater value is expected here because when applying a greater uncertainty, there is a larger advantage gained from optimising for it, (SA2 vs SA1 under 20% uncertainty). Despite this, under higher uncertainties, the mass of actual designs will be higher due to the more severe loadings (SA2 and SA1 under 20% vs 10% uncertainty). The difference in the mass of SA1 and SA2 designs indicates the current practice of designing for a fixed design loading using SAs with the 10% minimum ply percentage rule has merit, even when subject to an uncertain loading for which they have not been directly designed to carry.

In Fig. 8 (c) and (d) NSA laminates are designed for an uncertain loading (NSA2) and the largest mass saving over the current industrial practice (SA1) is seen to be 8.5%. In this comparison < 26% loadings allow > 5% mass saving for both ±10% and ±20% loading uncertainty. If uncertainty is designed for directly using both SA (SA2) and NSA (NSA2) then 100% of the mass savings from using NSAs compared to SAs are < 5% and at least 70% < 1%, see Figs. 8 (e) and (f). Hence, for a significant proportion of load cases, results indicate designing directly for uncertainty using SAs may reduce mass by the same amount as designing directly for uncertainty using NSAs. This implies, considering the cost associated with change and development of manufacturing processes required, use of NSAs may not be

worthwhile. However, as NSAs can match SA performance and for many load cases offer multiple equally optimal designs, their use may still be viable when designing for competing constraints e.g. manufacturing, damage tolerance or buckling resistance. The technique of designing directly for the uncertainty in loading also allows NSA laminates to be robust considering the lack of an equivalent 10% rule.

5. Conclusions

The normalised elastic energy derived from subjecting composite laminates to uncertain loading is used to compare design strategies for achieving minimum mass under the assumption of a fibre based failure. Designs employing non-standard angles ($0 \leq \theta \leq 180°$) are compared with standard angle (0°, ±45° and 90°) designs and the use of the industrially applied 10% minimum ply percentage rule in standard angle designs is compared to designing directly for an uncertainty in secondary loads of up to ±20% of the primary load.

Results from this study are the first to investigate the comparative robustness of standard and non-standard angles designs to an uncertain loading and indicate the potential for use of non-standard angles to reduce mass of future aircraft. It is shown that designing with non-standard angles for an uncertain design loading offers mass savings of up to 8.5%, compared to the current industry standard angle and design rule strategy. However, if design rules are ignored and standard angle laminates are also designed to carry uncertain loading directly, mass reduction through the use of non-standard angles is limited to less than 5% and is < 1% for a significant proportion of potential design loads. Laminate balancing about the principal loading axes, which effectively introduces non-standard angles in the manufacturing axes, is shown to allow up to ~20% mass saving for both standard and non-standard laminates and is particularly effective in dealing with the inefficiencies of laminate designs under shear.

Overall it is concluded that, non-standard angles exceed standard angle performance. However, given the additional cost and complexity of manufacture, for most load cases, a non-standard angle design is unwarranted. Indeed, in many cases balancing about principal loading axes is sufficient to convey the majority of any weight saving. Similarly, the widely used 10% rule is found to be effective in mitigating deleterious effects of uncertain loading especially when greater uncertainty is applied. Nevertheless, such conclusions only hold where laminate strength is not limited by resin dominated or structural (e.g. buckling) failure. In these cases, or where other design aspects become important, e.g. minimising manufacturing defects, non-standard ply angles may offer an advantage. For instance, the considerable

non-uniqueness of minimum mass non-standard angle designs, demonstrated in this study indicates non-standard angles offer enhanced scope for providing optimal stiffness properties whilst concurrently tailoring for other laminate requirements.

Acknowledgements

This work is part of the EPSRC ADAPT project (EP/N024354/1). Richard Butler is supported by a Royal Academy of Engineering/GKN Aerospace Research Chair in Composites Analysis.

References

1. Verchery G. The netting analysis as a limit case of the laminated structure theory. In: Proceedings of ICCM-19 Conference. Montreal, July, 2013. p. 1724-1731.
2. Niu MCY. Advanced composite structures. In: Niu MCY, editors. Airframe structural design - Practical design information and data on aircraft structures (2nd edition). Hong Kong: Conmilit Press Limited, 1999. p. 492-537.
3. Werter NPM, De Breuker R. Aeroelastic tailoring and structural optimisation using an advanced dynamic aeroelastic framework. In: Proceedings of IFASD 2015. Saint Petersburg, June, 2015. p. 1625-1644.
4. Shijun G, Wenyuan C, Degang C. Aeroelastic tailoring of composite wing structures by laminate layup optimization. AIAA J 2006;44(12):3146-3150.
5. Weaver PM, Bloomfield MW. On the potential for elastic tailoring in layered composites buckling considerations. In: Proceedings of ICCM-17 Conference. Edinburgh, July, 2009.
6. Diaconu CG, Sekine H. Layup optimization for buckling of laminated composite shells with restricted layer angles. AIAA J 2004;42(10):2153-2163.
7. York, CB. Tapered hygro-thermally curvature-stable laminates with non-standard ply orientations. Compos Part A: Appl Sci Manuf 2013;44:140-148.
8. Xia M, Takayanagi H, Kemmochi K. Analysis of multi-layered filament-wound composite pipes under internal pressure. Compos Struct 2001;53(4):483–491.
9. Kam TY, Liu YW, Lee FT. First-ply failure strength of laminated composite pressure vessels. Compos Struct 1997;38(1–4):65–70.

10. Elishakoff I, Haftka RT, Fang J. Structural design under bounded uncertainty—optimization with anti-optimization. Compos Struct 1994;53(6):1401-5.

11. Adali S, Lene F, Duvaut G, Chiaruttini V. Optimization of laminated composites subject to uncertain buckling loads. Compos Struct 2003;62(3-4):261-269.

12. Adali S. Design optimization of composite laminates under deterministic and uncertain conditions. In: Advani SG, Shonaike GO, editors. Advanced Polymeric Materials: Structure Property Relationships. Boca Raton: CRC Press, 2003. p.1-55.

13. Murotsu Y, Miki M, Shao S. Reliability design of fibre reinforced composites. Struct Safety 1994;15(1):35-49.

14. Abdalla MM, Kassapoglou C, Gürdal Z. Formulation of composite laminate robustness constraint in lamination parameters space. In: Proceedings of 50th AIAA/ASME/ASCE/AHS/ASC structures, structural dynamics, and materials conference. Palm Springs, May, 2009.

15. Peeters D, Abdalla M. Design guidelines in non-conventional composite laminate optimization. J Aircraft 2017;54(4),1454–1464.

16. Prager W, Taylor JE. Problems of optimal structural design. J Appl Mech 1968;35(1):102-106.

17. Pedersen P. On optimal orientation of orthotropic materials. Struct Optim 1989;1(2):101-106.

18. Nielsen M, Rhead AT, Butler R. Structural efficiency via minimisation of elastic energy in damage tolerant laminates. In: Proceedings of ECCM-16, Seville, June, 2014.

19. Katz KU, Katz MG, Kudryk T. Toward a clarity of the extreme value theorem. LU 2014;8(2):193-214.

20. MATLAB R2015b, MathWorks, 2015, Natick, MA.

21. Goldberg DE. Genetic algorithms in search, optimization and machine learning. Boston: Addison-Wesley Longman, 1989.

22. Conn AR, Gould NIM, Toint PL. A globally convergent augmented lagrangian algorithm for optimization with general constraints and simple bounds, SIAM J Numer Anal 1991;28(2);545-572.

23. Conn AR, Gould NIM, Toint PL. A globally convergent augmented lagrangian barrier algorithm for optimization with general inequality constraints and simple bounds. Math Comput 1997;66(217):261–288.

24. Caprino G, Visconti IC. A note on specially orthotropic laminates. J Compos Mater 1982, 16(5):395–399.

25. Nielsen MWD, Johnson K, Rhead AT, Butler R. Laminate design for optimised in-plane performance and ease of manufacture. Compos Struct 2017;177:119-128.

26. Miki M, Sugiyama Y. Optimum design of laminated composite plates using lamination parameters. AIAA J 1993;31(5):921-922.

Declaration of Interest

Funding: This work was supported by the EPSRC as part of the ADAPT project (EP/N024354/1). Richard Butler is supported by a Royal Academy of Engineering/GKN Aerospace Research Chair in Composites Analysis.